J|A|C|S
ARTICLES
Published on Web 01/29/2002

Phosphorus Chemical Shift Tensors of Phosphido Ligands in Ruthenium Carbonyl Compounds: ^{31}P NMR Spectroscopy of Single-Crystal and Powder Samples and ab Initio Calculations

Klaus Eichele,[†] Roderick E. Wasylishen,*[,†,‡] John F. Corrigan,[§] Nicholas J. Taylor,[§] Arthur J. Carty,[§] Kirk W. Feindel,[†,‡] and Guy M. Bernard[‡]

Contribution from the Department of Chemistry, Dalhousie University, Halifax, Nova Scotia, Canada B3H 4J3, the Department of Chemistry, University of Alberta, Edmonton, Alberta, Canada T6G 2G2, and the Guelph−Waterloo Centre for Graduate Work in Chemistry, Department of Chemistry, University of Waterloo, Waterloo, Ontario, Canada N2L 3G1

Received September 19, 2001

Abstract: The phosphorus chemical shift (CS) tensors of several ruthenium carbonyl compounds containing a phosphido ligand, μ-PR_2, bridging a Ru−Ru bond were characterized by solid-state ^{31}P NMR spectroscopy. As well, an analogous osmium compound was examined. The structures of most of the clusters investigated have approximate local C_{2v} symmetry about the phosphorus atom. Compared to the "isolated" PH_2^- anion, the phosphorus nucleus of a bridging phosphido ligand exhibits considerable deshielding. The phosphorus CS tensors of most of the compounds have spans ranging from 230 to 350 ppm and skews of approximately zero. Single-crystal NMR was used to investigate the orientation of the phosphorus CS tensors for two of the compounds, $Ru_2(CO)_6(\mu_2\text{-}\eta^2\text{-}C{\equiv}C{-}Ph)(\mu_2\text{-}PPh_2)$ and $Ru_3(CO)_9(\mu_2\text{-}H)(\mu_2\text{-}PPh_2)$. The intermediate component of the phosphorus CS tensor, δ_{22}, lies along the local C_2 axis in both compounds. The least shielded component, δ_{11}, lies perpendicular to the Ru−P−Ru plane while the most shielded component, δ_{33}, lies perpendicular to the C−P−C plane. The orientation of the phosphorus CS tensor for a third compound, $Ru_2(CO)_6(\mu_2\text{-}PPh_2)_2$, was investigated by the dipolar-chemical shift NMR technique and was found to be analogous, suggesting it to be the same in all compounds. Ab initio calculations of phosphorus magnetic shielding tensors have been carried out and reproduce the orientations found experimentally. The orientation of the CS tensor has been rationalized using simple frontier MO theory. Splittings due to ^{99,101}Ru−^{31}P spin−spin coupling have been observed for several of the complexes. A rare example of ^{189}Os−^{31}P spin−spin splittings is observed in the ^{31}P MAS NMR spectrum of the osmium cluster, where $^1J(^{189}\text{Os}, ^{31}\text{P})$ is 367 Hz. For this complex, the ^{189}Os nuclear quadrupolar coupling constant is on the order of several hundred megahertz.

Introduction

The diorganyl phosphido group, R_2P^-, is an excellent ligand in organometallic chemistry.[1] Although examples of terminally bonded phosphido ligands are known, so-called metallophosphines,[2] the vast majority of phosphido compounds features this ligand bridging two or more metals. This R_2P bridge is an extremely flexible, yet stable and generally unreactive entity, spanning a wide range of distances between bonding or nonbonding metal atoms. Phosphido complexes with M−P−M bond angles ranging from less than 70° to greater than 120° are known.[3] Considerable effort has been made to establish an empirical relationship of potential diagnostic value between the ^{31}P NMR chemical shift of the phosphido ligand and structural changes in bridges supporting bonding or nonbonding metals. For example, the presence or absence of metal−metal bonds has been found to have a pronounced effect on the ^{31}P chemical shift.[2a,e,3−6] Phosphorus chemical shifts of R_2P groups bridging M−M bonds are usually considerably larger than those of

* Corresponding author: (phone) 780-492-4336; (fax)780-492-8231; (e-mail) Roderick.Wasylishen@UAlberta.Ca.
[†] Dalhousie University.
[‡] University of Alberta.
[§] University of Waterloo.

(1) Mathey, F.; Sevin, A. *Molecular Chemistry of the Transition Elements*; John Wiley & Sons: Chichester, U.K., 1996; pp 144−145.
(2) (a) Lorenz, I.-P.; Mürschel, P.; Pohl, W.; Polborn, K. *Chem. Ber.* **1995**, *128*, 413−416. (b) Barré, C.; Boudot, P.; Kubicki, M. M.; Moïse, C. *Inorg. Chem.* **1995**, *34*, 284−291. (c) Malisch, R.; Barth, M.; Malisch, W. *J. Organomet. Chem.* **1984**, *260*, C35−C39. (d) Baker, R. T.; Whitney, J. F.; Wreford, S. S. *Organometallics* **1983**, *2*, 1049−1051. (e) Keiter, R. L.; Madigan, M. J. *Organometallics* **1982**, *1*, 409−411. (f) Baker, R. T.; Krusic, P. J.; Tulip, T. H.; Calabrese, J. C.; Wreford, S. S. *J. Am. Chem. Soc.* **1983**, *105*, 6763−6765. (g) Benac, B. L.; Cowley, A. H.; Jones, R. A.; Nunn, C. M.; Wright, T. C. *J. Am. Chem. Soc.* **1989**, *111*, 4986−4988.
(3) (a) Carty, A. J. *Adv. Chem. Ser.* **1982**, *196*, 163−193. (b) Carty, A. J.; Hartstock, F.; Taylor, N. J. *Inorg. Chem.* **1982**, *21*, 1349−1354. (c) Rosenberg, S.; Geoffroy, G. L.; Rheingold, A. L. *Organometallics* **1985**, *4*, 1184−1189. (d) Brauer, D. J.; Hessler, G.; Knüppel, P. C.; Stelzer, O. *Inorg. Chem.* **1990**, *29*, 2370−2375.
(4) Carty, A. J.; MacLaughlin, S. A.; Nucciarone, D. In *Phosphorus-31 NMR Spectroscopy in Stereochemical Analysis: Organic Compounds and Metal Complexes*; Verkade, J. G., Quin, L. D., Eds.; Methods in Stereochemical Analysis 8; VCH Publishers: Deerfield Beach, FL, 1987; pp 559−619.
(5) Bender, R.; Braunstein, P.; Dedieu, A.; Ellis, P. D.; Huggins, B.; Harvey, P. D.; Sappa, E.; Tiripicchio, A. *Inorg. Chem.* **1996**, *35*, 1223−1234.

corresponding coordinated phosphines, R_3P, while phosphorus nuclei in R_2P groups bridging nonbonding metals have smaller chemical shifts. These structural variations may cause phosphorus chemical shift differences of several hundred ppm. Precious little is known about the phosphorus chemical shift tensors of these complexes.

For a series of diiron hexacarbonyl complexes possessing an iron−iron bond, a phosphido bridge, and a second bridge of varying nature, an empirical correlation between the ^{31}P chemical shift measured in solution and the Fe−P−Fe angle has been proposed;[4] values of $\delta(^{31}P)$ range from ∼120 ppm for 70° to 200 ppm for 76°. Subsequent solid-state ^{31}P NMR studies[7] of powder samples of these compounds revealed that variations in δ_{11}, the principal component of the chemical shift tensor representing the direction of least shielding, are responsible for the trend in isotropic chemical shifts. Specifically, δ_{11} ranged from 240 to 460 ppm, while the principal components of intermediate and greatest shielding, δ_{22} and δ_{33}, varied between 120 and 180 ppm and between 5 and 75 ppm, respectively. Clearly, the influence of bond angles on phosphorus chemical shifts is highly directional, with δ_{11} being most sensitive to variations in the Fe−P−Fe angle. In contrast, the shielding experienced by phosphorus in systems lacking a metal−metal bond is characterized by values of δ_{33} that are large and negative.[7,8] For example, $\delta_{33} = -684$ ppm for the PHMes bridge (Mes = mesityl) in dinuclear platinum complexes.[8] Only a few other investigations of phosphorus chemical shift tensors in phosphido-bridging systems have appeared in the literature.[9]

The phosphorus chemical shifts of phosphido ligands bridging metal−metal bonds indicate that the phosphorus nuclei in these compounds are less shielded than in most classes of phosphorus compounds. In fact, only phosphinidene ligands, RP^{2-}, or unsaturated, low-coordinate phosphorus compounds exhibit less shielding.[10] In unsaturated compounds, the origin of the deshielding can generally be accounted for by an efficient mixing between orbitals arising from the lone-pair of electrons localized on phosphorus and low-lying unoccupied molecular orbitals of π-symmetry.[11] By using single-crystal ^{31}P NMR, we showed that in phosphinidene cluster compounds the direction of least shielding is parallel to the R−P bond.[12] A simple description of the frontier orbitals of the phosphinidene ligand is able to rationalize this finding in terms of mixing between the weakly bonding and antibonding π-type orbitals perpendicular to the R−P bond. In developing this interpretation, it was essential to have full knowledge of the three-dimensional nature of chemical shielding, i.e., magnitude and orientation of the chemical shift tensor components. So far, there is no information available about the orientation of phosphorus chemical shift tensors of phosphido groups.

Chart 1

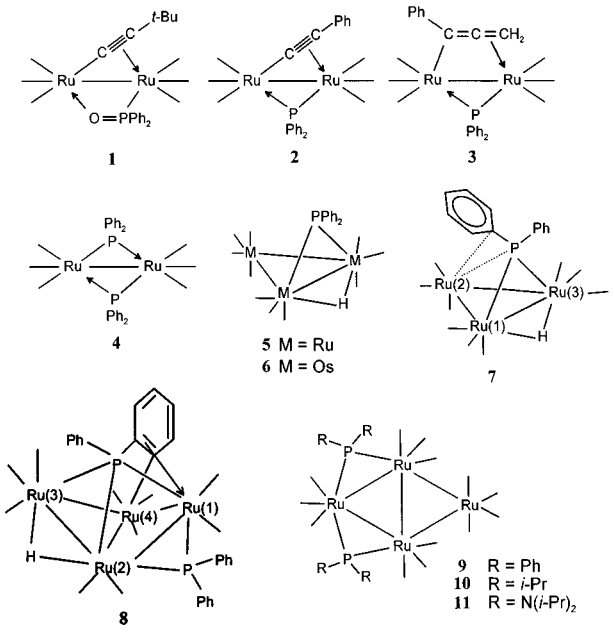

In the present study, our goal was to investigate ^{31}P chemical shift tensors of phosphido groups ligated to ruthenium or osmium carbonyl clusters (Chart 1). We have carried out solid-state ^{31}P NMR experiments on powder and single-crystal samples to experimentally characterize the magnitude and orientation of the phosphorus chemical shift tensors. Single-crystal ^{31}P NMR experiments have been performed on two of the compounds, **2** and **7**. Although the present investigation is experimental in nature, we also report the results of ab initio chemical shielding calculations performed on **2** and $Ru_2(CO)_6$-(μ_2-η^2-C≡C−*t*-Bu)(μ_2-PPh_2), and realistic models for **4** and **9**. Finally, we offer a simple rationalization of the observed chemical shift tensor orientations. Compound **4** has also been used as a model compound for the examination of the empirical correlation between the ^{31}P chemical shift and the metal−phosphorus−metal angle.

Experimental Section

Sample Preparation. The preparations of $Ru_2(CO)_6(\mu_2$-η^2-C≡C−*t*-Bu)(μ_2-PPh_2O)[13] (**1**), $Ru_2(CO)_6(\mu_2$-η^2-C≡C−Ph)(μ_2-PPh_2)[14] (**2**), $Ru_2(CO)_6(\mu_2$-η^3-Ph-C=C=CH_2)(μ_2-PPh_2)[15] (**3**), $Ru_2(CO)_6(\mu_2$-$PPh_2)_2$[16,17] (**4**), $Ru_3(CO)_{10}(\mu_2$-H)(μ_2-PPh_2)[18] (**5**), $Os_3(CO)_{10}(\mu_2$-H)(μ_2-PPh_2)[19] (**6**), $Ru_3(CO)_9(\mu_2$-H)(μ_2-PPh_2)[18,20] (**7**), $Ru_4(CO)_{10}(\mu_2$-H)(μ_2-PPh_2)[μ_4-η^2-

(6) Berger, S.; Braun, S.; Kalinowski, H.-O. *NMR Spectroscopy of the Non-Metallic Elements*; John Wiley & Sons: Chichester, England, 1997; pp 888−890.
(7) Carty, A. J.; Fyfe, C. A.; Lettinga, M.; Johnson, S.; Randall, L. H. *Inorg. Chem.* **1989**, *28*, 4120−4124.
(8) Kourkine, I. V.; Chapman, M. B.; Glueck, D. S.; Eichele, K.; Wasylishen, R. E.; Yap, G. P. A.; Liable-Sands, L. M.; Rheingold, A. L. *Inorg. Chem.* **1996**, *35*, 1478−1485.
(9) (a) Gobetto, R. *Mater. Chem. Phys.* **1991**. *29*, 221−233. (b) Randall, L. H.; Carty, A. J. *Inorg. Chem.* **1989**, *28*, 1194−1196.
(10) (a) Fluck, E.; Heckmann, G. In *Phosphorus-31 NMR Spectroscopy in Stereochemical Analysis: Organic Compounds and Metal Complexes*; Verkade, J. G., Quin, L. D., Eds.; VCH Publishers: Deerfield Beach, FL, 1987; pp 61−113. (b) Niecke, E.; Gudat, D. In *Phosphorus-31 NMR Spectral Properties in Compound Characterization and Structural Analysis*; Quin, L. D., Verkade, J. G., Eds.; VCH Publishers: New York, 1994; pp 159−174.
(11) (a) Zilm, K. W.; Webb, G. G.; Cowley, A. H.; Pakulski, M.; Orendt, A. *J. Am. Chem. Soc.* **1988**, *110*, 2032−2038. (b) Duchamp, J. C.; Pakulski, M.; Cowley, A. H.; Zilm, K. W. *J. Am. Chem. Soc.* **1990**, *112*, 6803−6809. (c) Curtis, R. D.; Schriver, M. J.; Wasylishen, R. E. *J. Am. Chem. Soc.* **1991**, *113*, 1493−1498. (d) Gudat, D.; Hoffbauer, W.; Niecke, E.; Schoeller, W. W.; Fleischer, U.; Kutzelnigg, W. *J. Am. Chem. Soc.* **1994**, *116*, 7325−7331. (e) Burford, N.; Cameron, T. S.; Clyburne, J. A. C.; Eichele, K.; Robertson, K. N.; Sereda, S.; Wasylishen, R. E.; Whitla, W. A. *Inorg. Chem.* **1996**, *35*, 5460−5467. (f) Wu, G.; Rovnyak, D.; Johnson, M. J. A.; Zanetti, N. C.; Musaev, D. G.; Morokuma, K.; Schrock, R. R.; Griffin, R. G.; Cummins, C. C. *J. Am. Chem. Soc.* **1996**, *118*, 10654−10655.
(12) Eichele, K.; Wasylishen, R. E.; Corrigan, J. F.; Taylor, N. J.; Carty, A. J. *J. Am. Chem. Soc.* **1995**, *117*, 6961−6969.
(13) (a) Fogg, D. E.; Carty, A. J. *Polyhedron* **1988**, *7*, 2285−2295. (b) Fogg, D. E.; Taylor, N. J.; Meyer, A.; Carty, A. J. *Organometallics* **1987**, *6*, 2252−2254.
(14) Cherkas, A. A.; Randall, L. H.; MacLaughlin, S. A.; Mott, G. N.; Taylor, N. J.; Carty, A. J. *Organometallics* **1988**, *7*, 969−977.
(15) (a) Carleton, N.; Corrigan, J. F.; Doherty, S.; Pixner, R.; Sun, Y.; Taylor, N. J.; Carty, A. J. *Organometallics* **1994**, *13*, 4179−4182. (b) Nucciarone, D.; Taylor, N. J.; Carty, A. J. *Organometallics* **1986**, *5*, 1179−1187.

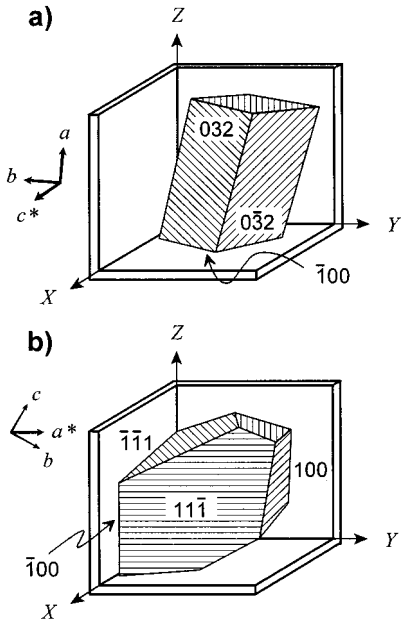

Figure 1. Relative orientations of the crystal axes (*a*, *b*, *c*) and NMR cube frame axes (*X*, *Y*, *Z*) for the single crystals employed in the ^{31}P single-crystal experiments on (a) **2** and (b) **7**.

P(Ph)C_6H_4]^{21} (**8**), $Ru_4(CO)_{13}(\mu_2$-$PPh_2)_2$^{22,23} (**9**), $Ru_4(CO)_{13}[\mu_2$-P(i-Pr)$_2]_2$^{23} (**10**), and $Ru_4(CO)_{13}\{\mu_2$-P[N(i-Pr)$_2]_2\}_2$^{23} (**11**) have been published previously.

2 crystallizes in the monoclinic space group $P2_1/c$, with $a = 9.512(2)$ Å, $b = 30.598(5)$ Å, $c = 9.831(2)$ Å, $\beta = 117.46(2)°$, and $Z = 4$.[14] A crystal of approximate dimensions $1.0 \times 2.5 \times 2.5$ mm^3 was chosen for the single-crystal NMR experiment. After indexing the crystal faces, the crystal was mounted on its $\bar{1}00$ face onto the *XY* plane of the crystal holder (Figure 1a) such that the crystal *a* and *b* axes are in the *YZ* plane, while *c** is parallel to *X*. **7** crystallizes in the monoclinic space group $P2_1/c$, with $a = 13.369(2)$ Å, $b = 11.824(1)$ Å, $c = 15.417(2)$ Å, $\beta = 97.32(1)°$, and $Z = 4$.[20] A crystal of approximate dimensions $2.0 \times 2.5 \times 3.5$ mm^3 was chosen for the single-crystal NMR experiment. After indexing the crystal faces, the crystal was mounted with its $\bar{1}00$ face on the *XZ* plane of the crystal holder (Figure 1b). This ensured that the crystal *b* and *c* axes are in the *XZ* plane with *a** parallel to *Y*.

The Euler angles necessary to transform from the cube frame to the orthogonalized crystal frame are $\alpha = 0°$, $\beta = 90°$, and $\gamma = 175°$ for **2** and $\alpha = 180°$, $\beta = 40°$, and $\gamma = 270°$ for **7**. These values were refined using the direction of the C_2 axis obtained from symmetry-related chemical shift tensors determined by the single-crystal NMR experiment (vide infra).

NMR Experiments. Solid-state ^{31}P NMR experiments were carried out at 81.03 MHz using a Bruker MSL-200 spectrometer ($B_0 = 4.7$ T). The single-crystal ^{31}P NMR spectra were obtained using an automated single-crystal goniometer probe from Doty Scientific. The cube mount was placed into a hollow cubic receptacle in the goniometer of the probe, with the rotation axis perpendicular to the magnetic field. Rotations about the three orthogonal cube axes *X*, *Y*, and *Z* were controlled by an external stepper motor placed underneath the probe. Spectra were acquired from 0° to 180° in 9° intervals for **2**. For **7**, intervals of 9° were used between 0° and 90° while 18° intervals were used for the second half of the rotation. The ^{31}P NMR spectra were acquired after cross-polarization (CP) using the Hartmann−Hahn match condition and under high-power proton decoupling, using ^{1}H $\pi/2$ pulse widths of 3.0 μs, contact times of 5 ms, and a flip-back pulse on the ^{1}H channel.[24] Recycle delays of 8 and 300 s, respectively were used for **2** and **7**. Typically, 80 (**2**) or 8 (**7**) FIDs were acquired, using a sweep width of 83 kHz and a time domain size of 2K. The ^{31}P NMR line widths were on average 280−350 Hz (**2**) or 350−400 Hz (**7**).

Phosphorus-31 CP NMR spectra of powder samples were acquired using a Bruker double-bearing magic-angle spinning (MAS) probe, with 3.0 μs proton $\pi/2$ pulse widths and contact times of 3−5 ms. Chemical shifts were referenced with respect to external 85% aqueous H_3PO_4 by setting the peak of external solid $NH_4H_2PO_4$ to 0.8 ppm. Analysis of spinning-sideband intensities in MAS NMR spectra was carried out using the program HBA, a nonlinear least-squares routine based on the Herzfeld−Berger method.[25] Calculations of ^{31}P MAS and static spectra, and for ^{31}P coupled to ^{99,101}Ru or ^{189}Os, were performed using WSolids; both programs were developed in our laboratory and run on IBM-compatible microprocessors.[26]

Molecular Orbital Calculations. Extended Hückel molecular orbital (EHMO) calculations were performed using the CACAO program with standard parameters.[27] The involvement of d orbitals on phosphorus was not considered. In all EHMO calculations, idealized models were used, based on the experimentally observed structures. The P−H bond length was fixed at 1.44 Å.[28]

Phosphorus chemical shielding tensors of H_2P^- were calculated using an efficient implementation[29] of the gauge-including atomic orbital (GIAO) method,[30] incorporated in the TEXAS 90 ab initio program package.[31] A 6-311G basis set was used, augmented with two sets of polarization functions on both types of atoms. The P−H bond distance was optimized at this level of theory, resulting in an equilibrium distance of 1.426 Å and an H−P−H angle of 93.68°. Absolute chemical shieldings were converted to chemical shifts using the absolute chemical shielding of 85% aqueous H_3PO_4, $\sigma = 328.35$ ppm.[32] Reported chemical shift values conform to the high-frequency positive convention. All shielding calculations were performed using an IBM RS6000/580 workstation.

Restricted Hartree−Fock (RHF) GIAO calculations were performed on **2**, $Ru_2(CO)_6(\mu_2$-η^2-C≡C−*t*-Bu)$(\mu_2$-$PPh_2)$, $Ru_2(CO)_6(\mu_2$-$PPh_2)(\mu_2$-$PMe_2)$ as a model for **4**, and $Ru_4(CO)_{13}(\mu_2$-$PPh_2)(\mu_2$-$PMe_2)$ as a model for **9** using the Gaussian 98W program[33] on a Dell Dimension XPS B866r PC. Experimental structures were used in all calculations, modified as indicated to allow for a reasonable calculation time. Phenyl hydrogens were added at a fixed C−H bond length of 1.08 Å.[34] Hydrogens were added to the methyl groups at a fixed bond length of 1.09 Å and bond angle of 109.5°. On models for **2** and **4**, phenyl rings

(16) (a) Corrigan, J. F.; Doherty, S.; Taylor, N. J.; Carty, A. J.; Boroni, E.; Tiripicchio, A. *J. Organomet. Chem.* **1993**, *462*, C24−C26. (b) He, Z.; Lugan, N.; Neibecker, D.; Mathieu, R.; Bonnet, J.-J. *J. Organomet. Chem.* **1992**, *426*, 247−259.
(17) Bullock, L. M.; Field, J. S.; Haines, R. J.; Minshall, E.; Moore, M. H.; Mulla, F.; Smit, D. N.; Steer, L. M. *J. Organomet. Chem.* **1990**, *381*, 429−456.
(18) (a) MacLaughlin, S. A.; Taylor, N. J.; Carty, A. J. *Organometallics* **1984**, *3*, 392−399. (b) Nucciarone, D.; MacLaughlin, S. A.; Carty, A. J. *Inorg. Synth.* **1989**, *26*, 264−268.
(19) (a) Nicholls, J. N.; Vargas, M. D. *Inorg. Synth.* **1989**, *26*, 289−293. (b) Colbran, S. B.; Johnson, B. F. G.; Lewis, J.; Sorrell, R. M. *J. Organomet. Chem.* **1985**, *296*, C1−C5. (c) Natarajan, K.; Zsolnai, L.; Huttner, G. *J. Organomet. Chem.* **1981**, *220*, 365−381.
(20) MacLaughlin, S. A.; Carty, A. J.; Taylor, N. J. *Can. J. Chem.* **1982**, *60*, 87−90.
(21) Corrigan, J. F.; Doherty, S.; Taylor, N. J.; Carty, A. J. *J. Am. Chem. Soc.* **1992**, *114*, 7557−7558.
(22) Hogarth, G.; Phillips, J. A.; Van Gastel, F.; Taylor, N. J.; Marder, T. B.; Carty, A. J. *J. Chem. Soc., Chem. Commun.* **1988**, 1570−1572.
(23) Corrigan, J. F.; Dinardo, M.; Doherty, S.; Hogarth, G.; Sun, Y.; Taylor, N. J.; Carty, A. J. *Organometallics* **1994**, *13*, 3572−3580.
(24) Tegenfeldt, J.; Haeberlen, U. *J. Magn. Reson.* **1979**, *36*, 453−457.
(25) Herzfeld, J.; Berger, A. E. *J. Chem. Phys.* **1980**, *73*, 6021−6030.
(26) Eichele, K.; Wasylishen, R. E. WSolids Ver. 1.17.30 and HBA Ver. 1.4.4, Dalhousie University, Halifax, 2001.
(27) Mealli, C.; Proserpio, D. M. *J. Chem. Educ.* **1990**, *67*, 399−402.
(28) Underwood, D. J.; Hoffmann, R.; Tatsumi, K.; Nakamura, A.; Yamamoto, Y. *J. Am. Chem. Soc.* **1985**, *107*, 5968−5980.
(29) Wolinski, K.; Hinton, J. F.; Pulay, P. *J. Am. Chem. Soc.* **1990**, *112*, 8251−8260.
(30) Ditchfield, R. *Mol. Phys.* **1974**, *27*, 789−807.
(31) Pulay, P. *Theor. Chim. Acta* **1979**, *50*, 299−312.
(32) Jameson, C. J.; De Dios, A.; Jameson, A. K. *Chem. Phys. Lett.* **1990**, *167*, 575−582.

Table 1. Phosphorus-31 Chemical Shift Tensor Components for Ruthenium and Osmium Carbonyl Phosphido Clusters **1**−**12**[a]

compound		δ_{iso}	δ_{11}	δ_{22}	δ_{33}	Ω
$Ru_2(CO)_6(\mu_2\text{-}\eta^2\text{-}C{\equiv}C{-}t\text{-}Bu)(\mu_2\text{-}PPh_2O)$	**1**	92.2[b]	205	96	−24	229
$Ru_2(CO)_6(\mu_2\text{-}\eta^2\text{-}C{\equiv}C{-}Ph)(\mu_2\text{-}PPh_2)$	**2**	129.3	256	128	2	254
$Ru_2(CO)_6(\mu_2\text{-}\eta^2\text{-}C{\equiv}C{-}i\text{-}Pr)(\mu_2\text{-}PPh_2)$[c]		135	269	143	−8	277
$Ru_2(CO)_6(\mu_2\text{-}\eta^2\text{-}C{\equiv}C{-}t\text{-}Bu)(\mu_2\text{-}PPh_2)$[c]		123.2	243	136	−10	253
$Ru_2(CO)_6(\mu_2\text{-}\eta^3\text{-}Ph\text{-}C{=}C{=}CH_2)(\mu_2\text{-}PPh_2)\cdot x CHCl_3$	**3′**	145.5	335	114	−12	347
$Ru_2(CO)_6(\mu_2\text{-}\eta^3\text{-}Ph\text{-}C{=}C{=}CH_2)(\mu_2\text{-}PPh_2)$	**3**	140.8	329	110	−17	346
$Ru_2(CO)_6(\mu_2\text{-}PPh_2)_2$	**4**	114.1[d]	269	113	−39	308
$Ru_3(CO)_{10}(\mu_2\text{-}H)(\mu_2\text{-}PPh_2)$	**5**	131.7[e]	292	98	5	287
$Os_3(CO)_{10}(\mu_2\text{-}H)(\mu_2\text{-}PPh_2)$	**6**	14.0[f]	141	−13	−86	227
$Ru_3(CO)_9(\mu_2\text{-}H)(\mu_2\text{-}PPh_2)$	**7**	130.4	233	127	33	200
$Ru_4(CO)_{10}(\mu_2\text{-}H)(\mu_2\text{-}PPh_2)[\mu_4\text{-}\eta^2\text{-}P(Ph)C_6H_4]$	**8**	220.4[g]	457	176	28	429
		38.5	188	−12	−60	248
$Ru_4(CO)_{13}(\mu_2\text{-}PPh_2)_2$	**9**	117.4[h]	244	149	−41	285
		114.4[h]	242	151	−49	291
$Ru_4(CO)_{13}[\mu_2\text{-}P(i\text{-}Pr)_2]_2\cdot CHCl_3$	**10′**	151.6[i]	320	157	−22	342
		149.1[i]	304	162	−19	323
$Ru_4(CO)_{13}[\mu_2\text{-}P(i\text{-}Pr)_2]_2$	**10**	156.8[i]	323	168	−21	344
		142.1[i]	292	156	−22	314
$Ru_4(CO)_{13}\{\mu_2\text{-}P[N(i\text{-}Pr)_2]_2\}_2$	**11**	231.2	370	230	100	270
$Ru_8(CO)_{21}(\mu_6\text{-}P)(\mu_4\text{-}PPh)(\mu_2\text{-}PPh_2)$	**12**[j]	214.3	562	139	−58	620

[a] In ppm with respect to external aqueous 85% H_3PO_4. Errors in the isotropic chemical shift, $\delta_{iso} = (\delta_{11} + \delta_{22} + \delta_{33})/3$, are estimated to be 0.5 ppm, errors in the principal components, $\delta_{11} \geq \delta_{22} \geq \delta_{33}$, are estimated to be 2−4% of the span of the chemical shift tensor, $\Omega = \delta_{11} - \delta_{33}$. [b] $^1J(^{99}Ru,^{31}P) = 100$ Hz, $d = -22$ Hz. [c]Reference 7. [d]Euler angles relating the chemical shift tensors to the dipolar frame of reference: $\alpha = 0, \beta = 90, \gamma = \pm 25°$. [e] $^1J(^{99}Ru,^{31}P) = -92$ Hz. [f] $^1J(^{187}Os,^{31}P) = 108$ Hz in solution. [g] $^1J(^{99}Ru,^{31}P) = 172$ Hz, ref 56. [h] $^2J(^{31}P,^{31}P) = 69$ Hz. [i] $^2J(^{31}P,^{31}P) = 60-70$ Hz. [j]Reference 12; the values quoted are for the μ_2-PPh_2 group.

on one phosphorus atom were replaced by methyl groups, maintaining the P−C bond length to the ipso carbon.

Calculations were performed using locally dense basis sets; a 6-311G diffuse basis set, augmented with two sets of polarization functions on phosphorus and directly bonded atoms; an effective core potential (ECP), LANL2DZ, for transition metals; and 3-21G was employed for the remainder of the molecule. Absolute chemical shieldings have been converted to chemical shifts as stated above.

Results and Discussion

The phosphorus chemical shift tensors obtained from powder and single-crystal samples of compounds **1**−**11** (Chart 1) are summarized in Tables 1−3, together with data on the phosphido group in **12**, obtained in our study of phosphinidene groups.[12] The results of the ab initio calculations of phosphorus chemical shift tensors are collected in Table 4. First, we shall discuss the spectra of powder samples obtained for the different types of cluster compounds, followed by the single-crystal ^{31}P NMR results. Next, the results from the ab initio calculations are discussed and finally a qualitative interpretation of our experimental findings is offered.

Phosphorus Chemical Shift Tensors from Powder Studies. The ^{31}P NMR spectra of powder samples of $Ru_2(CO)_6(\mu_2\text{-}\eta^2\text{-}C{\equiv}C{-}t\text{-}Bu)(\mu_2\text{-}PPh_2O)$ (**1**) are shown in Figure 2. The principal components of the ^{31}P chemical shift tensor may be retrieved either from the characteristic frequencies of the powder pattern of a stationary sample (Figure 2a) or from analysis of the spinning-sideband intensities[25] in a slow-spinning MAS spectrum (Figure 2b). The phosphorus environment of the phosphidoxo bridge in **1** may be described as being between that of a metallophosphine oxide[2a,b] and a phosphido-bridging system;[35] therefore, the chemical shift tensor may be expected to exhibit characteristics of both. For typical tertiary phosphine oxides, the hemipolar P−O bond usually dominates the phosphorus shielding.[36] Generally, the phosphorus chemical shift tensors are essentially axially symmetric, and furthermore, the substituent effects are relatively small, with principal components of $\delta_{\parallel} \approx -50$ to -100 ppm, while $\delta_{\perp} \approx 100$ ppm. In the present complex, this symmetry is lost; however, the value of δ_{22}, 96 ppm, is approximately equal to $\delta_{\perp}$ while $\delta_{33} \approx \delta_{\parallel}$. The most profound change occurs for δ_{11}. This component, $\delta_{11} = 205$ ppm, is clearly larger than in ordinary phosphine oxides. While

Table 2. Linear Least-Squares Coefficients (in ppm) Obtained from the Single-Crystal ^{31}P NMR Experiments on Compounds **2** and **7**[a]

compd	site	rot.	*A*	*B*	*C*
2	(1)	*X*[b]	94.0(6)	63.4(7)	65.3(8)
		Y	113.0(5)	−83.7(6)	16.8(7)
		Z[c]	176.9(2)	19.7(3)	−64.7(4)
	(2)	*X*[b]	90.3(4)	79.6(6)	−37.0(6)
		Y	107.8(4)	−98.9(5)	11.7(6)
		Z[c]	188.1(1)	19.1(2)	58.8(2)
7	(1)	*X*	132.7(3)	69.2(4)	71.1(4)
		Y	96.0(5)	−31.8(6)	−3.1(7)
		Z[d]	161.2(2)	−34.7(2)	1.4(2)
	(2)	*X*	160.4(3)	36.9(3)	2.5(4)
		Y	101.5(1)	22.2(2)	−18.0(2)
		Z[d]	134.7(4)	−55.2(5)	−82.3(6)

[a] Standard deviations in units of least significant digits are given in parentheses. [b]Phase angle, 1.5°. [c]Phase angle, 3.0°. [d]Phase angle, 4.0°.

(33) Frisch, M. J.; Trucks, G. W.; Schlegel, H. B.; Scuseria, G. E.; Robb, M. A.; Cheeseman, J. R.; Zakrzewski, V. G.; Montgomery, J. A., Jr.; Stratmann, R. E.; Burant, J. C.; Dapprich, S.; Millam, J. M.; Daniels, A. D.; Kudin, K. N.; Strain, M. C.; Farkas, O.; Tomasi, J.; Barone, V.; Cossi, M.; Cammi, R.; Mennucci, B.; Pomelli, C.; Adamo, C.; Clifford, S.; Ochterski, J.; Petersson, G. A.; Ayala, P. Y.; Cui, Q.; Morokuma, K.; Malick, D. K.; Rabuck, A. D.; Raghavachari, K.; Foresman, J. B.; Cioslowski, J.; Ortiz, J. V.; Stefanov, B. B.; Liu, G.; Liashenko, A.; Piskorz, P.; Komaromi, I.; Gomperts, R.; Martin, R. L.; Fox, D. J.; Keith, T.; Al-Laham, M. A.; Peng, C. Y.; Nanayakkara, A.; Gonzalez, C.; Challacombe, M.; Gill, P. M. W.; Johnson, B.; Chen, W.; Wong, M. W.; Andres, J. L.; Gonzalez, C.; Head-Gordon, M.; Replogle, E. S.; Pople, J. A. *Gaussian 98*, revision A.7; Gaussian, Inc.: Pittsburgh, PA, 1998.
(34) Jeffrey, G. A.; Ruble, J. R.; McMullan, R. K.; Pople, J. A. *Proc. R. Soc. London A* **1987**, *414*, 47.
(35) Corrigan, J. F.; Taylor, N. J.; Carty, A. J. *J. Chem. Soc., Chem. Commun.* **1994**, 1769−1770.
(36) (a) Eichele, K.; Wasylishen, R. E.; Kessler, J. M.; Solujić, L.; Nelson, J. H. *Inorg. Chem.* **1996**, *35*, 3904−3912. (b) Robert, J. B.; Wiesenfeld, L. *J. Magn. Reson.* **1980**, *38*, 357−360. (c) Grimmer, A.-R.; Müller, D. *Z. Chem.* **1976**, *16*, 244, 496−497. (d) Grimmer, A.-R. *Z. Chem.* **1978**, *18*, 233.

Table 3. Orientation of the ^{31}P Chemical Shift Tensor in the Crystal Axis Frame for Compounds **2** and **7** as Determined by Single-Crystal ^{31}P NMR Spectroscopy[a]

compd		δ_{ii} (ppm)	*a*	*b*	*c**
2[b]	δ_{11}	255.7(18)	−0.1842(87)	0.6203(77)	0.7624(84)
	δ_{22}	127.6(30)	0.2562(85)	−0.7185(62)	0.6466(103)
	δ_{33}	1.8(1)	0.9489(6)	0.3145(11)	−0.0266(84)
			*a**	*b*	*c*
7[b]	δ_{11}	233.3(53)	−0.9142(8)	0.3342(15)	0.2294(56)
	δ_{22}	126.8(4)	−0.1173(77)	−0.7597(35)	0.6396(55)
	δ_{33}	33.1(1)	0.3880(43)	0.5578(6)	0.7337(66)

[a] Reported for crystallographic site 1. To obtain the direction cosines for site 2, the symmetry operation $\bar{x}y\bar{z}$ should be carried out. Standard deviations in units of least significant digits are given in parentheses. [b]The NMR site 2 (cf. Table 2) has been assigned to crystallographic site 1.

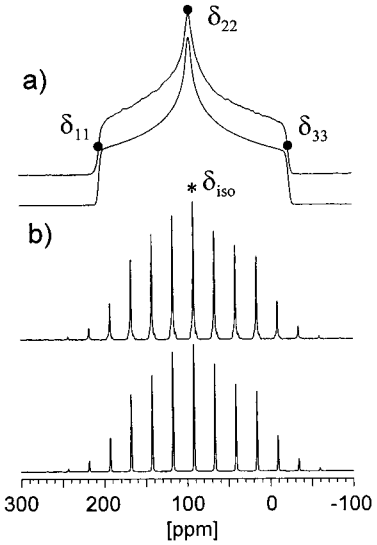

Figure 2. Experimental and calculated ^{31}P NMR spectra of powder samples of **1**, obtained at 4.7 T. (a) Spectra of a stationary powder sample, with the positions of the chemical shift tensor principal components indicated in the experimental spectrum (upper trace). (b) Spectra obtained at a spinning rate of 3.14 kHz. The isotropic peak is indicated by an asterisk. Weak satellites due to coupling with ^{101,99}Ru, visible in the experimental spectrum (upper trace, cf. Figure 11a), have not been included in the simulation (lower trace).

δ_{33} is generally directed along the P−O bond in most phosphine oxides, this may not be the case in **1**, because the approximate local symmetry of **1** is much lower than for typical R_3PO compounds.

The compound $Ru_2(CO)_6(\mu_2\text{-}\eta^2\text{-}C{\equiv}C{-}Ph)(\mu_2\text{-}PPh_2)$ (**2**) is the first real phosphido bridging system that we discuss, although the principal components of the phosphorus chemical shift tensor are similar to the previous example. This compound was also subjected to a single-crystal ^{31}P NMR investigation, to be discussed in the next section. The principal components reported in Table 1, obtained from powder and single-crystal samples, are in good agreement with the values obtained by Carty et al.[7] using the method of moments: $\delta_{11} = 249$ ppm, $\delta_{22} = 139$ ppm, and $\delta_{33} = 1$ ppm. Also investigated in the latter study were compounds with other substituents, $Ru_2(CO)_6(\mu_2\text{-}\eta^2\text{-}C{\equiv}C{-}R)(\mu_2\text{-}PPh_2)$ with R = *i*-Pr and *t*-Bu (Table 1). Individual principal components of the phosphorus chemical shift tensors exhibit variations on the order of 20 ppm,[7] even though the substituent R is several angstroms from phosphorus.

Upon recrystallizing $Ru_2(CO)_6(\mu_2\text{-}\eta^3\text{-}Ph\text{-}C{=}C{=}CH_2)(\mu_2\text{-}PPh_2)$ (**3**) from chloroform, the product exists as the chloroform solvate, **3′**, which eventually releases the solvent to yield pure **3**. Therefore, the ^{31}P CP/MAS NMR spectrum exhibits two sites, the ratio of which changed after several weeks. The principal components of the phosphorus chemical shift tensor of each species, **3** and **3′**, are not significantly different.

As the prototype of ruthenium phosphido complexes, $Ru_2(CO)_6(\mu_2\text{-}PPh_2)_2$ (**4**) has been known since 1972[37] but has not been readily available until recently.[16b,38] The crystal structure of **4** consists of two independent molecules within the asymmetric unit, with all four phosphorus atoms being crystallographically distinct.[17] However, their structural features are identical within experimental error: Ru−P−Ru angles of 73.3(1), 73.3(1), 73.8(1), and 73.8(1)° and C−P−C angles between 99.2 and 99.8°. Overall, the molecular symmetry approaches C_{2v} as in the related cyclohexyl-substituted ruthenium compound, $Ru_2(CO)_6(\mu_2\text{-}PCy_2)_2$,[38] and an iron analogue.[39] The ^{31}P CP/MAS spectrum obtained with a spinning rate of 6.0 kHz shows one relatively broad (150 Hz) isotropic peak. Because the four distinct phosphorus sites in **4** cannot be resolved in the ^{31}P MAS spectrum at $B_0 = 4.7$ T, we will consider them crystallographically equivalent at this field. The chemical shift tensors of crystallographically equivalent nuclei have the same principal components and hence the same isotropic shift. However, unless such nuclei are related by a center of inversion, the orientation of their principal axes differs and they are magnetically nonequivalent. As a consequence, they may exhibit different chemical shifts for some orientations of the molecule in the applied magnetic field (vide infra). The two ^{31}P nuclei within one molecule of **4** are 2.983(5) Å apart, which results in a ^{31}P,^{31}P direct dipolar coupling constant, $R = (\mu_0/4\pi)(\gamma^2/r^3)(\hbar/2\pi)$, of 743(4) Hz. This interaction causes additional features in the spectrum of a static powder sample (see Figure 3) as compared to a pure chemical shift anisotropy powder pattern (e.g., see Figure 2). In the case of isolated spin pairs, dipolar splittings are observed about the frequencies corresponding to the principal components of the chemical shift tensor. We shall classify spin systems as A_2 or AX spin systems, depending on whether they consist of magnetically equivalent nuclei or nuclei that differ significantly in their resonance frequencies, respectively.[40] In the case of **4**, additional humps and dips are evident (Figure 3a), implying that at some orientations the spin system is neither A_2 nor AX but rather AB.[41] Analysis of the spectrum indicates that δ_{33} is perpendicular to the internuclear vector; the splitting about δ_{33} is 1100 Hz, corresponding to an effective dipolar coupling constant of

(37) Bruce, M. I.; Shaw, G.; Stone, F. G. A. *J. Chem. Soc., Dalton Trans.* **1972**, 2094−2099.
(38) (a) Béguin, A.; Dai, M. C.; Laurenczy, G.; Rheinwald, G.; Roulet, R.; Stoeckli-Evans, H.; Süss-Fink, G.; Tabacchi, R. *J. Organomet. Chem.* **1997**, *527*, 167−172. (b) Béguin, A.; Böttcher, H.-C.; Süss-Fink, G.; Walther, B. *J. Chem. Soc., Dalton Trans.* **1992**, 2133−2134.
(39) Ginsburg, R. E.; Rothrock, R. K.; Finke, R. G.; Collman, J. P.; Dahl, L. F. *J. Am. Chem. Soc.* **1979**, *101*, 6550−6562.
(40) Eichele, K.; Wasylishen, R. E. *J. Magn. Reson. Ser. A* **1994**, *106*, 46−56.

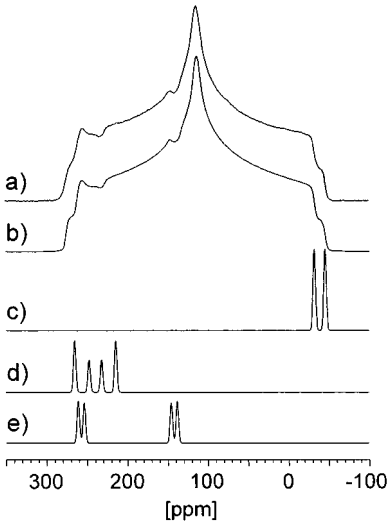

Figure 3. Experimental (a) and calculated (b−e) ^{31}P NMR spectra of powder samples of **4**, obtained at 4.7 T. The two upper traces show spectra of a stationary powder sample, with additional features due to homonuclear spin−spin interactions clearly visible. The lower traces show theoretical spectra of individual molecules with different orientations in the external magnetic field. The orientations were chosen such that the phosphorus nuclei of the homonuclear spin pair behave as an A_2 (c), AB (d), or AX (e) spin system.

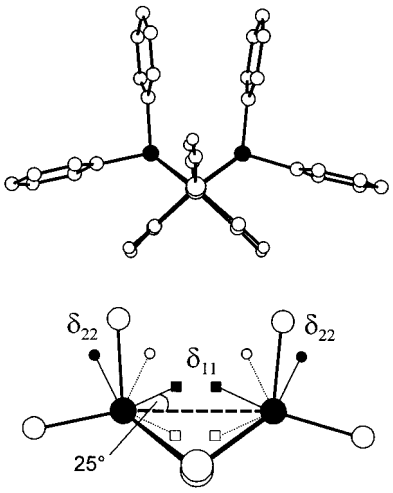

Figure 4. Perspective view of a molecule of **4** and the orientation of the phosphorus chemical shift tensors in the molecular frame of reference as determined from analysis of the dipolar-chemical shift powder pattern shown in Figure 3 and by considering the local symmetry about phosphorus. Two alternative assignments result. In both cases, the direction of highest shielding, δ_{33}, is perpendicular to the paper plane. The two assignments differ by the orientation of δ_{11} being 25° above or below the internuclear vector, indicated by a solid or open square, and analogously for δ_{22}, shown as solid or open circles.

733 Hz. This value is in excellent agreement with the value calculated from the known internuclear separation, 743 Hz. Furthermore, δ_{11} makes an angle of 25° with the direction of the internuclear vector. Given that the approximate local symmetry about phosphorus is C_{2v}, two possible orientations for the phosphorus chemical shift tensor in the molecular frame of reference arise, as illustrated in Figure 4. The small "peak" at 147 ppm (Figure 3) is quite sensitive to the orientation of δ_{11} with respect to the internuclear vector; deviations from 25° by as little as 1° can be detected easily.

To account for the presence of the humps and dips observed in the ^{31}P NMR spectrum of **4** (Figure 3a), particularly those at about 147 and 240 ppm, consider a single crystallite at specific orientations, as illustrated in Figure 3c−e. The spectrum in Figure 3c results when the applied magnetic field, B_0, is perpendicular to the paper plane of Figure 4 and, hence, parallel to δ_{33} of both phosphorus nuclei. At this orientation, their chemical shifts are identical and they constitute an A_2 spin system. With B_0 perpendicular to the internuclear vector, the dipolar splitting of 1100 Hz corresponds to $(3/2)R$. For the next trace, Figure 3d, B_0 is within the paper plane of Figure 4, only 8° off the ^{31}P,^{31}P internuclear vector. This causes a slight chemical shift difference in the two phosphorus sites and the homonuclear dipolar coupling is close to its maximum value of $3R$. A spectrum similar to an AB spin system arises for this orientation, with unequal peak heights causing dips and humps to appear in the powder pattern. Finally, if B_0 is close to δ_{11} for one of the phosphorus nuclei (40° off the internuclear vector), it will be close to δ_{22} for the second nucleus. The resulting large chemical shift difference causes the spectrum to approach the AX limit of a two-spin system (Figure 3e).

The dipolar splittings observed in the spectrum shown in Figure 3 yield two possible solutions for the orientations of the phosphorus chemical shift tensors in the molecular frame (see Figure 4). The mutual orientation of the phosphorus chemical shift tensors depicted with solid lines and symbols is the one preferred, because it is in better agreement with orientations obtained for the related compounds **2** and **7** from the single-crystal ^{31}P NMR studies, and it agrees well with ab initio calculations (vide infra). In the alternative assignment of the phosphorus shift tensor orientation, δ_{11} would bisect the C−P−C angle and δ_{22} would be perpendicular to the Ru−P−Ru plane. The preferred assignment indicates a significant reduction of the local approximate C_{2v} symmetry about phosphorus toward C_s. This reduction in the local symmetry is possibly caused by the presence of a second phosphorus atom ~3 Å away. Notably, even a regular single-crystal ^{31}P NMR experiment would be unable to distinguish between the two assignments shown in Figure 4 unless an additional dipolar interaction, for example, with an NMR active isotope of the metal, were to provide a second internal frame of reference.

Compounds **5**−**8** represent successive steps in the transformation of phosphido clusters into phosphinidene clusters via activation of phenyl groups.[42] Compound **5** and its osmium analogue, **6**, are regular phosphido complexes; the loss of a carbonyl group in **7** induces an additional weak P−Ph interaction of the phosphido bridge with the coordinatively unsaturated Ru(2). Taken a step further, cluster **8** features a pentacoordinate phosphido bridge where one of the phenyl groups is ortho-metalated and η^2-bound. The data in Table 1 demonstrate that these structural changes are reflected in the principal components of the phosphorus chemical shift tensors of these compounds. As a typical phosphido cluster, **5** does not exhibit any irregularities in its phosphorus chemical shift tensor. However, of interest is the comparison with its osmium analogue, **6**. The phosphorus

(41) (a) Zilm, K. W.; Grant, D. M. *J. Am. Chem. Soc.* **1981**, *103*, 2913−2922. (b) Curtis, R. D.; Hilborn, J. W.; Wu, G.; Lumsden, M. D.; Wasylishen, R. E.; Pincock, J. A. *J. Phys. Chem.* **1993**, *97*, 1856−1861. (c) Eichele, K.; Ossenkamp, G. C.; Wasylishen, R. E.; Cameron, T. S. *Inorg. Chem.* **1999**, *38*, 639−651.

(42) Cherkas, A. A.; Corrigan, J. F.; Doherty, S.; MacLaughlin, S. A.; van Gastel, F.; Taylor, N. J.; Carty, A. J. *Inorg. Chem.* **1993**, *32*, 1662−1670.

isotropic shift of the latter is more than 100 ppm toward lower frequency compared to **5**. This change in the isotropic chemical shift is the result of a global shift of all three principal components toward lower frequencies. Such heavy-atom shifts on light nuclei are not uncommon. A theoretical account of their origin has been the subject of several recent papers.[43]

The loss of one CO in **5** to give **7** does not seem to affect the isotropic phosphorus chemical shift, but the values of the principal components of the chemical shift tensor indicate this to be the result of fortuitous cancellation of changes in individual components. A shift in δ_{11} by 60 ppm to lower frequency is compensated by opposite shifts in δ_{22} and δ_{33}. For **7**, we carried out a single-crystal ^{31}P NMR study, to be discussed below.

A rare example of a pentacoordinate phosphido bridge is present in **8**. This cluster is fluxional in solution, with a hydrogen atom exchanging between the Ru(2)−Ru(3) and Ru(3)−Ru(4) bonds.[21] At 298 K, two averaged ^{31}P signals were observed at 214.3 (μ-PPh_2) and 59.6 ppm ({C_6H_4}PPh), but at 193 K, four peaks were observed with δ values of 211.8 and 38.3 ppm (isomer A) and 199.3 and 91.6 ppm (isomer B). Given the chemical shifts measured in the solid state, 220.4 and 38.5 ppm (Table 1), and the known crystal structure,[21] we can assign isomer A to the structure where H bridges the Ru(2)−Ru(3) bond. Cluster **8** is actually prepared from **9**. The low-frequency shift of the {C_6H_4}PPh group, $\delta_{iso} = 38.5$ ppm, is indicative of the unusual, severe structural rearrangement. In contrast, the phosphido group bridging the Ru(1)−Ru(2) bond experiences an unusual shift to high frequency. Of the PPh_2 groups listed in Table 1, the ^{31}P nucleus in **8** is the least shielded. The reduction of the bridged Ru(1)−Ru(2) distance on going from 3.178 Å in **9** to 2.829 Å in **8**, in combination with a reduction of the Ru−P−Ru angle from 85.9° to 76.6°, may account for this observation.

The clusters **9**−**11** represent electron-rich 64-electron systems of planar, rhomboidal Ru_4 units. The intriguing structural properties of these compounds have been discussed previously.[21,22,44] As a consequence of their electron richness, these molecules exhibit elongation of one or more of the Ru−Ru bonds, with accompanying widening of the Ru−P−Ru angles, 81.8−86.0°. According to the empirical ^{31}P chemical shift−structure correlation outlined in the Introduction, such widening should result in deshielding of the phosphorus nucleus; however, this is not the case. The most deshielded phosphorus is that of **11** and it has the smallest Ru−P−Ru angle. However, one should keep in mind that the change in the Ru−P−Ru bond angles is actually caused by quite different substituents on phosphorus. The direct effect of these substituents on ^{31}P chemical shifts may mask any secondary effects due to bond angle changes. For example, it is known for organyl phosphines that an amino substituent causes stronger deshielding than an isopropyl or a phenyl group. All three principal components of the ^{31}P chemical shift tensor for **11** are shifted to higher values by 80−145 ppm compared to the corresponding phenyl-substituted compound. In contrast, the isopropyl substituent of **10** affects primarily δ_{11} compared to the phenyl analogue, **9**.

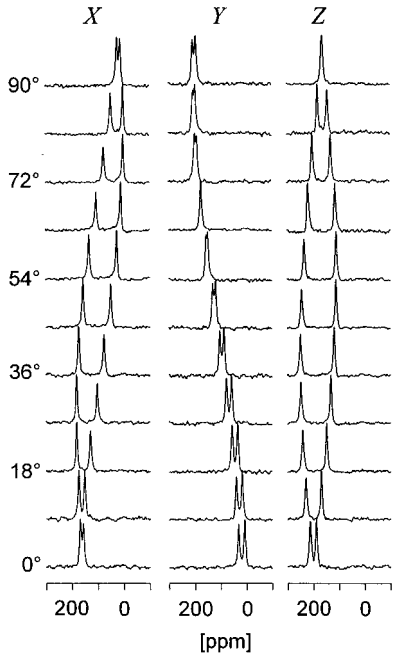

Figure 5. Phosphorus-31 NMR spectra of a single crystal of **2** as a function of crystal orientation in the external magnetic field. Rotations were performed consecutively about the cube *X*, *Y*, *Z* axes (Figure 1) in 9° increments.

For all three clusters, the phosphorus chemical shifts are relatively large, consistent with the unusual structures of these flat butterfly clusters. While the phosphorus nuclei of **9** and **10** are chemically equivalent in solution, they are crystallographically nonequivalent in the solid state. This makes it straightforward to measure $^2J(^{31}P,^{31}P)$. Values in the range 60−70 Hz were obtained from the ^{31}P CP/MAS NMR spectra of **9**, **10**, and its chloroform solvate **10′** (Table 1). Peaks in spectra of **11** are broadened by residual ^{31}P−^{14}N spin−spin interactions and do not show resolved splittings due to $^2J(^{31}P,^{31}P)$.

Single-Crystal ^{31}P NMR of Clusters 2 and 7. Both compounds contain only one phosphorus atom and their crystals belong to the same space group; hence, they are discussed together. Details of the analysis of single-crystal NMR spectra are given elsewhere.[45] Qualitatively, as the orientation of the single crystal is changed about an axis perpendicular to the external magnetic field, the chemical shift varies in a sinusoidal fashion. The precise manner in which the chemical shift varies depends on the orientation and magnitude of the principal components of the chemical shift tensor. Thus, tracing the NMR frequency of a particular site through three orthogonal rotations allows for the characterization of the symmetric part of the chemical shift tensor. Spectra of **2** and **7** as a function of crystal orientation in the magnetic field are shown in Figure 5 and Figure 6, respectively. For both compounds, two ^{31}P NMR peaks were generally observed for any given orientation of the crystal in the applied magnetic field. The unit cells of both **2** and **7** contain four crystallographically equivalent molecules. They are pairwise related via a center of inversion, which makes them magnetically equivalent. The nuclei in sites related to each other via the C_2 operation are magnetically nonequivalent, giving rise

(43) (a) Vaara, J.; Ruud, K.; Vahtras, O. *J. Chem. Phys.* **1999**, *111*, 2900−2909. (b) Ruiz-Morales, Y.; Schreckenbach, G.; Ziegler, T. *J. Phys. Chem.* **1996**, *100*, 3359−3367. (c) Kaupp, M.; Malkin, V. G.; Malkina, O. L.; Salahub, D. R. *Chem. Eur. J.* **1996**, *2*, 24−30. (d) Li, J.; Schreckenbach, G.; Ziegler, T. *Inorg. Chem.* **1995**, *34*, 3245−3252.

(44) Corrigan, J. F.; Dinardo, M.; Doherty, S.; Carty, A. J. *J. Cluster Sci.* **1992**, *3*, 313−332.

(45) (a) Power, W. P.; Mooibroek, S.; Wasylishen, R. E.; Cameron, T. S. *J. Phys. Chem.* **1994**, *98*, 1552−1560. (b) Eichele, K.; Wasylishen, R. E. *J. Phys. Chem.* **1994**, *98*, 3108−3113. (c) Eichele, K.; Wu, G.; Wasylishen, R. E.; Britten, J. F. *J. Phys. Chem.* **1995**, *99*, 1030−1037. (d) Kennedy, M. A.; Ellis, P. D. *Concepts Magn. Reson.* **1989**, *1*, 35−47, 109−129.

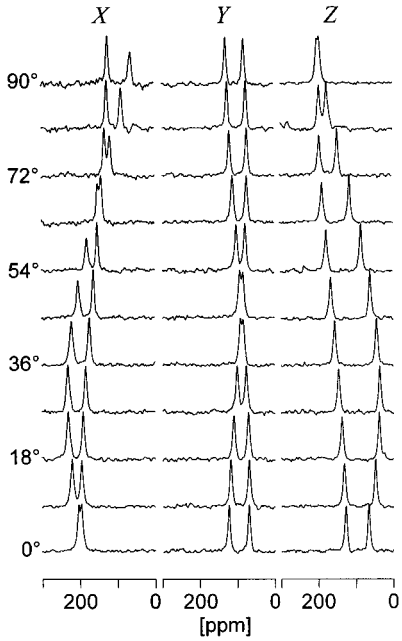

Figure 6. Phosphorus-31 NMR spectra of a single crystal of **7** as a function of crystal orientation in the external magnetic field. Rotations were performed consecutively about the cube *X*, *Y*, *Z* axes (Figure 1) in 9° increments.

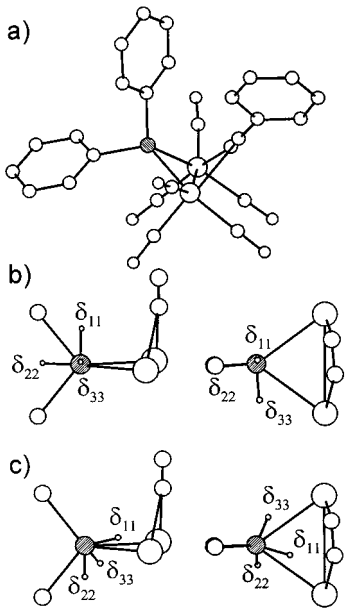

Figure 7. The two possible orientations of the ^{31}P chemical shift tensors in the molecular frame of reference of **2**. (a) A perspective drawing of **2**. (b) Two different views of the assignment preferred here, clearly reflecting the local symmetry, while (c) shows two views of the alternative assignment.

to two peaks in general. For orientations where the C_2 axis is parallel to the external magnetic field, all four molecules become equivalent, giving rise to a single peak. Also, the crystal of **2** has its C_2 (*b* axis) almost parallel to *Y*; therefore, the rotation about *Y* shows two closely spaced peaks (Figure 5).

Observed peak positions, $\delta_i(\varphi)$, as a function of rotation progress, φ, about the cube axis *i* were fit to a general equation of type

$$\delta_i(\varphi) = A_i + B_i \cos 2\varphi + C_i \sin 2\varphi \qquad (1)$$

using a linear least-squares procedure. The resulting nine coefficients from the three rotations $i = X, Y, Z$, given in Table 2, were used to construct the chemical shift tensors in the cube frame. After diagonalization, the principal components of the chemical shift tensors and their direction cosines in the cube frame were obtained. Using the symmetry relationships between the crystallographically equivalent but magnetically nonequivalent chemical shift tensors, the Euler angles defining the crystal orientation in the cube frame were refined. For **2**, the refined Euler angles are $\alpha = 3°$, $\beta = 90°$, and $\gamma = 174°$; the orientations of the symmetry-related principal components differ by less than 4°. For **7**, the refined Euler angles are $\alpha = 176°$, $\beta = 41°$, and $\gamma = 270°$; in this case, the orientations of symmetry-related tensors differ by less than 1°. The maximum difference in the orientation of symmetry-related tensors is a measure of the internal consistency of our data. These refined Euler angles were used to transform the chemical shift tensors into the crystal axis frame (Table 3). The assignment of the magnetically nonequivalent tensors to specific crystallographic sites is impossible based on the single-crystal NMR data alone.[46] Based on the local molecular symmetry about phosphorus, approximately C_{2v}, one expects that the orientation of the principal components reflects this symmetry. This is illustrated for **2** and **7** in Figure 7 and Figure 8, respectively. In each case, one assignment reflects the local symmetry rather well, while the other assignment does not reflect the local symmetry in any way. Also, it is worth pointing out that for both compounds the assignments with the anticipated local symmetry have essentially the same orientation. Specifically, the direction of least shielding, corresponding to δ_{11}, is oriented perpendicular to the Ru−P−Ru plane, while the direction of greatest shielding, δ_{33}, lies normal to the C−P−C plane. The bisector of both the Ru−P−Ru and C−P−C angle defines the orientation of the intermediate principal component of the shift tensor. Even though there are in principle two solutions possible from the analysis of the single-crystal data, the fact that the two independent single-crystal experiments yield analogous orientations provides strong support for the preferred orientations shown in Figure 7 and Figure 8. These assignments are also supported by the ab initio calculations on a model for **2**.

Phosphorus Chemical Shift Tensors from Ab Initio Calculations. To resolve the ambiguities in the orientations of the phosphorus chemical shift tensors in **2**, **4**, and **7**, we have performed ab initio calculations. The chemical shift tensors calculated for **2**, $Ru_2(CO)_6(\mu_2\text{-}\eta^2\text{-}C{\equiv}C{-}t\text{-}Bu)(\mu_2\text{-}PPh_2)$, $Ru_2(CO)_6(\mu_2\text{-}PPh_2)(\mu_2\text{-}PMe_2)$ as a model for **4**, and $Ru_4(CO)_{13}(\mu_2\text{-}PPh_2)(\mu_2\text{-}PMe_2)$ as a model for **9** are compared to experimental values in Table 4. In general, the differences between experimental and calculated principal components are on the order of 20−30 ppm but can be as large as 70 ppm. Most important, the results of the calculations enable us to resolve the ambiguities in assigning the experimentally determined shift tensor orientations.

For **2**, the difference angles between the preferred experimental and calculated shift tensor orientations are 16° (δ_{11}, δ_{22}) and 22° (δ_{33}), strongly supporting the orientation favored in Figure 7. Similarly, the calculated orientation for **4** places δ_{11} above the internuclear vector (cf. Figure 4), forming an angle

(46) Haeberlen, U. In *High-Resolution NMR in Solids, Selective Averaging*; Waugh, J. S., Ed.; Advances in Magnetic Resonance, Suppl. 1; Academic Press: New York, 1976.

Table 4. Observed and Calculated[a] Phosphorus-31 Chemical Shift Tensor Components[b] for Ruthenium Carbonyl Clusters

compound			δ_{iso}	δ_{11}	δ_{22}	δ_{33}	Ω	κ[c]
$Ru_2(CO)_6(\mu_2\text{-}\eta^2\text{-}C{\equiv}C{-}Ph)(\mu_2\text{-}PPh_2)$	**2**	exp	129	256	128	2	254	−0.008
		calc	107	190	98	32	158	−0.165
		calc[d]	113	201	101	38	163	−0.227
$Ru_2(CO)_6(\mu_2\text{-}\eta^2\text{-}C{\equiv}C{-}t\text{-}Bu)(\mu_2\text{-}PPh_2)$[e]		exp	123	243	136	−10	253	0.154
		calc	101	184	100	20	164	−0.024
$Ru_2(CO)_6(\mu_2\text{-}PPh_2)_2$	**4**	exp	114	269	113	−39	308	−0.013
$Ru_2(CO)_6(\mu_2\text{-}\boldsymbol{P}Ph_2)(\mu_2\text{-}PMe_2)$[f]		calc	113	252	96	−10	262	−0.191
$Ru_4(CO)_{13}(\mu_2\text{-}PPh_2)_2$	**9**	exp	117	244	149	−41	285	0.333
		exp	114	242	151	−49	291	0.375
$Ru_4(CO)_{13}(\mu_2\text{-}\boldsymbol{P}Ph_2)(\mu_2\text{-}PMe_2)$[f]		calc	101	172	154	−24	196	0.816

[a] Calculated at the RHF 6-311++G(2d,2p) level for phosphorus and directly bonded atoms, LANL2DZ ECP on ruthenium, and 3-21G for remainder of molecule. [b] In ppm with respect to external aqueous 85% H_3PO_4. Shieldings have been converted to shifts using $\delta = 328.35$ ppm $- \sigma$. [c] Skew of chemical shift tensor, $\kappa = 3(\delta_{22} - \delta_{iso})/\Omega$. [d] With 6-311++G(3d,3p) on phosphorus and directly bonded atoms; the C≡C−Ph group has been replaced with C≡C−Me. [e] Reference 7. [f] A smaller basis set has been used for the phosphorus of the PMe_2 group; thus, these phosphorus chemical shifts are not reported here.

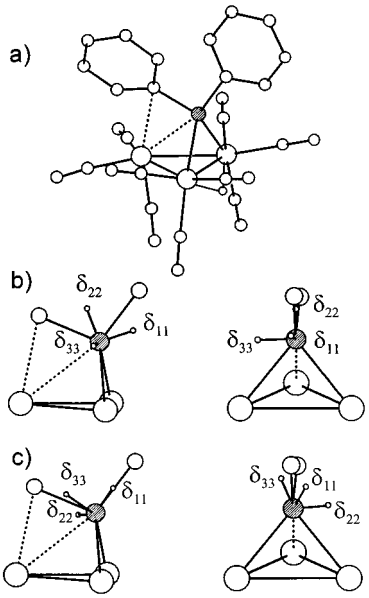

Figure 8. The two possible orientations of the ^{31}P chemical shift tensors in the molecular frame of reference of **7**. (a) A perspective drawing of **7**. (b) Two different views of the assignment preferred here, clearly reflecting the local symmetry, while (c) shows two views of the alternative assignment.

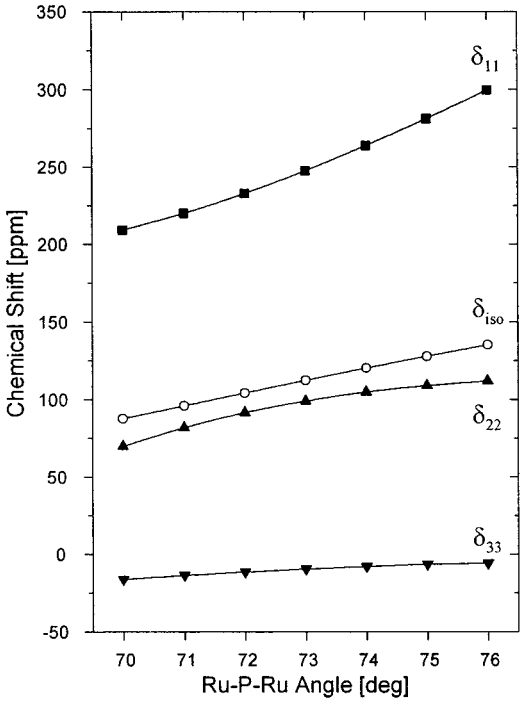

Figure 9. Ab initio calculation results for the model of **4**, examining the dependence of the phosphorus chemical shift tensor on the metal−phosphorus−metal angle.

of 19° with this direction and 34° with the normal to the Ru−P−Ru plane, indeed indicating a degradation of the local C_{2v} symmetry toward C_s. Thus, δ_{33} makes an angle of 4° with the normal to the C−P−C plane. In contrast, the local symmetry approximation holds quite well in the case of $Ru_4(CO)_{13}(\mu_2\text{-}PPh_2)(\mu_2\text{-}PMe_2)$, a model for **9**. The direction of least shielding is perpendicular to the Ru−P−Ru plane, forming an angle of 6° with the normal to this plane, while δ_{33} is perpendicular to the C−P−C plane, only 3° off the normal to this plane. In summary, a consistent orientation for the phosphorus chemical shift tensor in ruthenium phosphido clusters has been established.

Compound $Ru_2(CO)_6(\mu_2\text{-}PPh_2)(\mu_2\text{-}PMe_2)$ was used as a model to study the effect of Ru−P−Ru bond angle changes on the phosphorus chemical tensor. The results displayed in Figure 9 parallel the empirical correlation between the Fe−P−Fe bond angle and ^{31}P chemical shift found for a series of diiron hexacarbonyl phosphido complexes.[7] Values of δ_{iso} were found to range from ∼88 ppm for 70° to 135 ppm for 76°. The trend in isotropic chemical shifts depends strongly on δ_{11}, showing values ranging from 209 to 300 ppm, while δ_{22} and δ_{33} vary between 70 and 111 ppm and between −16 and −6 ppm, respectively. A general deshielding trend is evident for all tensor components as the Ru−P−Ru bond angle increases, in agreement with experimental observations.[7]

Interpretation of Phosphorus Chemical Shift Tensors. As shown by the data summarized in Table 1, the principal components of the phosphorus chemical shift tensors of phosphido groups in ruthenium carbonyl clusters span a relatively large range, generally more than 200 ppm and up to ∼600 ppm (**12**, discussed in a previous study[12]). This large anisotropy primarily arises from δ_{11}, a significant deshielding that results when B_0 is approximately perpendicular to the Ru−P−Ru triangle, as shown by our single-crystal and dipolar-chemical shift data. In the following discussion, we shall provide a qualitative rationalization for this observation.

The original theory of Ramsey[47] is useful in providing a qualitative interpretation of chemical shielding and hence chemical shifts. Following this theory, the shielding experienced

(47) Ramsey, N. F. *Phys. Rev.* **1950**, *78*, 699−703; **1952**, *86*, 243−246.

by a nucleus is given as the sum of a diamagnetic and a paramagnetic term. The diamagnetic term is always positive and hence leads to shielding, while the paramagnetic term, σ^p, is generally negative and leads to deshielding. For nuclei such as phosphorus, it is generally accepted that it is the paramagnetic term that is mainly responsible for *variations* in chemical shielding.[48]

Following the perturbation treatment of Ramsey, the magnitude of σ^p increases as the mixing of high-lying occupied and low-lying empty orbitals is facilitated by a decreasing energy separation between them. Mixing of orbitals, however, is only allowed if their symmetries follow selection rules analogous to magnetic dipole-allowed transitions.[49] Qualitatively, the magnitude of σ^p along a particular direction depends on efficient mixing of orbitals in a plane perpendicular to that direction.[48] Finally, the MOs will only make a large contribution to σ^p at the observed nucleus if the AOs centered on that nucleus have large coefficients in these MOs. This is reflected in the observation that chemical shielding is most sensitive to the local environment. For these reasons, we are primarily interested in MOs with major contributions from phosphorus and shall restrict our interpretation to the frontier MOs (FMOs) of the phosphido unit, H_2P^-, and consider their interactions with other molecular fragments. Similar simplified interpretations were successful in explaining phosphorus chemical shielding tensors of phosphinidene ruthenium clusters[12] and have also been used to rationalize carbon chemical shielding tensors for methylene units bridging diiron compounds[50] and the nitrogen chemical shifts of imido ligands in mononuclear transition metal complexes.[51]

The FMOs of the H_2P^- group may conveniently be described as consisting of a 3p-type lone pair perpendicular to the plane of the phosphido group and an sp^2-type lone pair in the plane of the H_2P^- fragment. Such FMOs are isolobal[52] to those of H_2C^{2-} and, according to their symmetry, are commonly referred to as π- and σ-type orbitals (Figure 10). There are also σ- and σ^*-orbitals associated with the P−H bond. Compared to other phosphorus compounds, the highly deshielded phosphorus nuclei of bridging phosphido groups imply that the energy separation between occupied and empty orbitals is of major importance. On the other hand, the simple MO scheme for an isolated H_2P^- unit (Figure 10) suggests that the phosphorus nucleus of this species is very shielded. In the direction perpendicular to the H_2P^- fragment, only magnetic dipole-allowed mixing of the π-type lone pair with the σ^* MO of the P−H bond contributes to σ^p. Indeed, our GIAO calculations show that the principal components of the chemical shift tensor are $\delta_{11} = -185$ ppm (parallel to the C_2 axis), $\delta_{22} = -304$ ppm (perpendicular to the H−P−H plane), and $\delta_{33} = -538$ ppm, ($\delta_{iso} = -342$ ppm, $\Omega = 353$ ppm). We and others[53] have carried out several calculations using different methods and basis sets; the results are qualitatively consistent.

The phosphido group found in most transition metal compounds generally bridges two metal atoms which are part of a cluster and hence contain formal metal−metal bonds. To discuss the results of our single-crystal NMR experiments, we shall consider the interaction of an H_2P^- fragment with a binuclear metal fragment. The σ-type orbital of the H_2P^- ligand can effectively overlap with the M−M bond of the cluster frame. The phosphorus π-type orbital may simultaneously overlap with orbitals from two metal atoms. For the approximate C_{2v} clusters considered here, the bonding and antibonding orbitals resulting from the phosphorus σ, π, and P−H orbitals belong to the irreducible representations a_1, b_1, and b_2, respectively. In Figure 10, arrows indicate magnetic dipole-allowed mixing of occupied and unoccupied orbitals, along with their polarization. The relative energies were obtained from EHMO calculations on $Ru_2(CO)_6(\mu_2\text{-}PH_2)_2$. This qualitative scheme can be used to rationalize the orientation of the phosphorus shielding tensor found for **2**, **4**, and **7**. Indeed, we believe that it can be applied to all the clusters studied here and all diorganyl phosphido groups that bridge metal−metal bonds. The least shielded direction is predicted to be perpendicular to the PRu_2 plane and is the result of efficient mixing of occupied and unoccupied orbitals associated with the metal−phosphorus bonds; these orbitals are separated by the smallest energy gap. The most shielded direction is perpendicular to the PR_2 plane. It should be noted that the highest occupied and lowest unoccupied orbitals involving phosphorus do not necessarily correspond to the HOMO and LUMO of the total cluster.

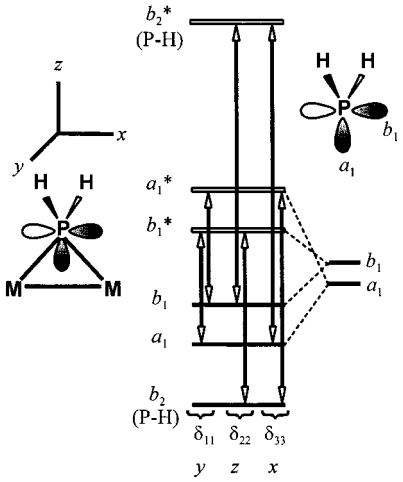

Figure 10. Frontier orbitals of a phosphido unit interacting with a dinuclear metal cluster fragment. The magnetic dipole-allowed mixing between occupied and unoccupied orbitals, together with the direction of this mixing, is indicated. These directions correspond to the orientations of the principal components of the chemical shift tensor.

As indicated in the Introduction, systems without metal−metal bonds are generally highly shielded. Such an observation cannot simply be accounted for by the energy gap and suggests strongly that other factors must become important. In this respect, phosphido groups differ from phosphinidene groups, which invariably show deshielding. Obviously, a detailed explanation has to await more thorough theoretical investigations.

Phosphorus−Metal Spin−Spin Interactions. For complexes **1**−**5** and **7**−**11**, the phosphorus of the phosphido group bridges at least two ruthenium carbonyl fragments, whereas in **6** it bridges two osmium fragments. Both of these metals have two naturally occurring NMR active isotopes; however, except for ^{187}Os, they are quadrupolar nuclei. ^{99}Ru: $I = {}^5/_2$, n.a. = 12.7%,

(48) Jameson, C. J.; Gutowsky, H. S. *J. Chem. Phys.* **1964**, *40*, 1714−1724.
(49) Schatz, G. C.; Ratner, M. A. *Quantum Mechanics in Chemistry*; Prentice Hall: Englewood Cliffs, NJ, 1993; pp 92−95.
(50) Kim, A. J.; Altbach, M. I.; Butler, L. G. *J. Am. Chem. Soc.* **1991**, *113*, 4831−4838.
(51) Bradley, D. C.; Hodge, S. R.; Runnacles, J. D.; Hughes, M.; Mason, J.; Richards, R. L. *J. Chem. Soc., Dalton Trans.* **1992**, 1663−1668.
(52) Hoffmann, R. *Angew. Chem., Int. Ed. Engl.* **1982**, *21*, 711−724.
(53) Caputo, M. C.; Ferraro, M. B.; Bochicchio, R. C.; Lazzeretti, P.; Malagoli, M.; Zanasi, R. *J. Mol. Struct.* **1993**, *287*, 77−88.

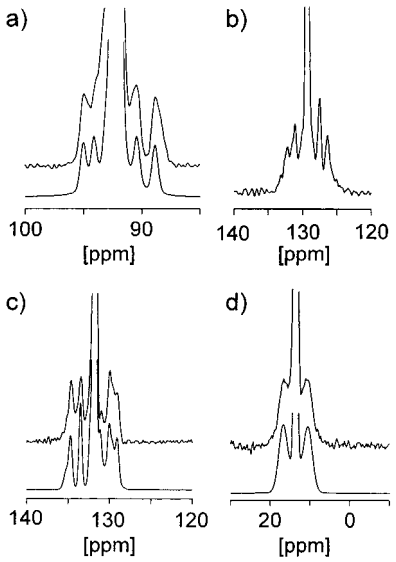

Figure 11. Expansions of ^{31}P CP/MAS NMR spectra obtained at 4.7 T and processed using a slight resolution enhancement, showing the isotropic regions with ^{99,101}Ru,^{31}P or ^{187,189}Os,^{31}P spin−spin interactions resolved. The upper portion of the isotropic peaks has been clipped to illustrate the satellites. (a) **1**, clipped at 10%; (b) **2**, clipped at 20%; (c) **5**, clipped at 20%; (d) **6**, clipped at 10%.

$\gamma = -1.2286 \times 10^7$ rad s^{-1} T^{-1}, $Q = 0.079 \times 10^{-28}$ m^2. ^{101}Ru: $I = {}^5/_2$, n.a. = 17.0%, $\gamma = -1.3771 \times 10^7$ rad s^{-1} T^{-1}, $Q = 0.457 \times 10^{-28}$ m^2. ^{187}Os: $I = {}^1/_2$, n.a. = 1.6%, $\gamma = 0.6193 \times 10^7$ rad s^{-1} T^{-1}. ^{189}Os: $I = {}^3/_2$, n.a. = 16.1%, $\gamma = 2.1071 \times 10^7$ rad s^{-1} T^{-1}, $Q = 0.856 \times 10^{-28}$ m^2.[54] Compared to ^{99}Ru, both ^{101}Ru and ^{189}Os possess large quadrupole moments, Q. On the other hand, the magnetogyric ratio of ^{189}Os is ∼3.4 times larger than that of ^{187}Os. The solid-state MAS NMR spectra of spin-$^1/_2$ nuclei, which are spin−spin coupled to a quadrupolar nucleus, may exhibit splittings and line shapes that depend on the sign and magnitude of the nuclear quadrupolar coupling constant, C_Q, the electric field gradient (EFG) asymmetry parameter, η_Q, the orientation of the EFG tensor relative to the internuclear vector, the effective dipolar coupling constant between the two spins, and the indirect spin−spin coupling constant, J. The influence of quadrupolar nuclei on spin-$^1/_2$ NMR spectra has been reviewed.[55] Previously, we provided the first examples of ^{99,101}Ru,^{31}P spin−spin coupling, inter alia for **8**;[56] the interested reader can also find an outline of the relevant theory there. We have observed further evidence of ^{99,101}Ru,^{31}P spin−spin coupling in the ^{31}P MAS spectra of all ruthenium clusters studied here; however, in most cases the satellites were not resolved well enough for a detailed analysis. The greatest problem in analyzing the multiplets is associated with the general lack of reliable ruthenium quadrupolar coupling constant data (C_Q and η_Q values).[56] So far, there are only some data obtained indirectly, either from our earlier ^{31}P MAS studies[56] or from ^{99}Ru NMR relaxation data in solution.[57]

An expansion of the isotropic region in the ^{31}P MAS spectrum of **1**, Figure 11a, clearly demonstrates the presence of ^{99,101}Ru satellites. In the case at hand, the intensities of the satellites indicate that ^{31}P interacts only with the ruthenium to which it is directly bonded. A detailed analysis is, at present, not possible because application of first-order theory is probably not strictly valid; however, a tentative estimate of $|^1J(^{99,101}\text{Ru},^{31}\text{P})|$ gives 100 ± 20 Hz. Examples of even more complicated patterns will be discussed for some of the other compounds.

Although the principal components of the phosphorus chemical shift tensor of **2** are not too different from those of **1**, clear differences arise in the satellite spin−spin coupling pattern (Figure 11b). For **2**, both Ru−P distances are the same within experimental error, but the ruthenium atoms are chemically different. Considering the ^{31}P,Ru,Ru spin system, a complex mixture of ruthenium isotopomers results: (i) Ru($I = 0$), Ru($I = 0$) = 49.3%, (ii) two isotopomers, Ru($I = 0$),^{99}Ru and ^{99}Ru,Ru($I = 0$), with 8.9% each; (iii) two isotopomers, Ru($I = 0$),^{101}Ru and ^{101}Ru,Ru($I = 0$), with 12.0% each, and (iv) higher isotopomers accounting for 8.9% of the total intensity. From the intensities of the satellites, each of these isotopomers appears to contribute to the observed spectrum, but the total spectrum is too complex to be analyzed.

The ^{31}P MAS NMR spectrum of **5** also exhibits satellites due to coupling with ruthenium (Figure 11c). Similar to **2**, the multiplet consists of several isotopomers. The two Ru−P distances for the monoclinic crystals are the same within experimental error, 2.354(1) Å,[58] as has been observed for the related cluster having PHPh fragments, 2.338(1) and 2.339(1) Å.[59] Assuming both ruthenium atoms of the bridge are equivalent, the experimental spectrum has been simulated using $R(^{99}\text{Ru},^{31}\text{P}) = -171$ Hz, $^1J(^{99}\text{Ru},^{31}\text{P}) = -92$ Hz, $C_Q(^{99}\text{Ru}) = 8$ MHz, $\eta_Q = 0$, and $\beta = 49°$. To obtain the ruthenium eigenstates in generating this theoretical spectrum, it was necessary to diagonalize the combined quadrupolar and Zeeman Hamiltonian for ruthenium. Also, it was assumed that the EFG tensors at Ru are axially symmetric. Slight deviations between the simulated and experimental spectra may arise because the ruthenium atoms are not equivalent and because of the assumption that $\eta_Q = 0$.

The ^{31}P MAS NMR spectrum of **6** also shows satellites (Figure 11d). While ^{187}Os ($I = {}^1/_2$) satellites have been observed previously in solution ^{31}P NMR spectra,[60,61] satellites arising from ^{189}Os ($I = {}^3/_2$) are absent because of extremely efficient quadrupolar relaxation in solution. In contrast, the satellites in the solid-state ^{31}P NMR spectra mainly originate from the more abundant but quadrupolar ^{189}Os nuclei, which have relatively long relaxation times in the solid state. In fact, the solution ^{31}P NMR spectrum of **6** shows ^{187}Os satellites with a $^1J(^{187}\text{Os},^{31}\text{P})$ of 108 Hz, which is somewhat greater than the $^1J(^{187}\text{Os},^{31}\text{P})$ observed for octahedral pentaosmium phosphinidene clusters, 77 Hz.[61] The splittings in the ^{31}P MAS NMR spectrum of **6** can be simulated using an approach similar to that for **5**, with

(54) Mills, I.; Cvitaš, T.; Homann, K.; Kallay, N.; Kuchitsu, K. *Quantities, Units and Symbols in Physical Chemistry*, 2nd ed.; International Union of Pure and Applied Chemistry; Blackwell Science Ltd.: Oxford, U.K., 1993.
(55) (a) Harris, R. K.; Olivieri, A. C. *Prog. NMR Spectrosc.* **1992**, *24*, 435−456. (b) Harris, R. K. In *Encyclopedia of Nuclear Magnetic Resonance*; Grant, D. M., Harris, R. K., Eds.; John Wiley & Sons: Chichester, U.K., 1996; Vol. 4, pp 2909−2914. (c) McDowell, C. A. In *Encyclopedia of Nuclear Magnetic Resonance*; Grant, D. M., Harris, R. K., Eds.; John Wiley & Sons: Chichester, U.K., 1996; Vol. 4, pp 2901−2908.
(56) Eichele, K.; Wasylishen, R. E.; Corrigan, J. F.; Doherty, S.; Sun, Y.; Carty, A. J. *Inorg. Chem.* **1993**, *32*, 121−123.
(57) Granger, P.; Richert, T.; Elbayed, K.; Kempgens, P.; Hirschinger, J.; Raya, J.; Rosé, J.; Braunstein, P. *Mol. Phys.* **1997**, *92*, 895−902.
(58) van Gastel, F. Ph.D. Dissertation, University of Waterloo, 1991.
(59) Iwasaki, F.; Mays, M. J.; Raithby, P. R.; Taylor, P. L.; Wheatly, P. J. *J. Organomet. Chem.* **1981**, *213*, 185−206.
(60) (a) Bell, A. G.; Koźmiński, W.; Linden, A.; von Philipsborn, W. *Organometallics* **1996**, *15*, 3124−3135. (b) Gill, D. F.; Mann, B. E.; Masters, C.; Shaw, B. L. *J. Chem. Soc., Chem. Commun.* **1970**, 1269.
(61) Colbran, S. B.; Johnson, B. F. G.; Lewis, J.; Sorrell, R. M. *J. Chem. Soc., Chem. Commun.* **1986**, 525−527.

$^1J(^{189}Os,^{31}P) = 367$ Hz, calculated from $^1J(^{187}Os,^{31}P)$, $R = 280$ Hz,[19b] $\alpha = 90°$, $\beta = 50°$, $C_Q(^{189}Os) = 1000$ MHz, and $\eta_Q = 0.5$. Note that for ^{189}Os the Zeeman interaction is only a small perturbation on the quadrupolar interaction. The value of C_Q should not be taken too literally, but stands for the fact that a C_Q several orders of magnitude larger (>300 MHz) than the Zeeman frequency, $\nu_0(^{189}Os) = 15.762$ MHz at $B_0 = 4.7$ T, is required to change the four-line multiplet due to indirect spin−spin coupling to an $I = {}^3/_2$ nucleus into what appears as a doublet. Other examples of coupling to quadrupolar nuclei with very large quadrupolar coupling constants have been reported for ^{197}Au and ^{201}Hg.[62]

Conclusions

The results presented here constitute the first experimental characterization of the orientation of phosphorus chemical shift tensors for the phosphido moiety. Comparison with results from RHF GIAO ab initio calculations indicates that these calculations show great promise in their ability to reproduce experimentally obtained tensor values even in this challenging class of compounds. In particular, the calculations have proven to be very useful in the confirmation of experimentally obtained chemical shift tensor orientations. Presently, the results for the bridging phosphido groups have been qualitatively rationalized using a simple molecular orbital model. However, now that the reliability of the ab initio calculations has been established, these methods will present a powerful tool for examining correlations between NMR chemical shift and molecular structure and gaining a deeper understanding of the factors which give rise to these observed trends.

Acknowledgment. We thank the Natural Sciences and Engineering Research Council of Canada (NSERC) for financial assistance in the form of equipment and operating grants (R.E.W., A.J.C.). We thank Professor Peter Pulay for providing us with the TEXAS software, and David Bryce, Dr. Myrlene Gee, and Dr. Michael Lumsden for valuable discussions. All solid-state NMR spectra were recorded at the Atlantic Region Magnetic Resonance Centre, which is also supported by NSERC. R.E.W. is a Canada Research Chair in Physical Chemistry at the University of Alberta.

JA0122041

(62) Angermair, K.; Bowmaker, G. A.; de Silva, E. N.; Healy, P. C.; Jones, B. E.; Schmidbaur, H. *J. Chem. Soc., Dalton Trans.* **1996**, 3121−3129.